Statistical analysis

All data were expressed as mean±S.E.M. Differences between vehicle- and rotenone-treated groups were tested for significance by one- or two-way analysis of variance (ANOVA) followed by a post hoc Dunnett test. Differences between the rotenone-treated groups and the respective time-matched untreated group were tested for significance by two-tailed Student's *t*-test. A *P* value less than 0.05 denoted the presence of a statistically significant difference.

RESULTS

Rotenone induces dopaminergic neuronal cell death and neurite retraction

In order to estimate the percentage of different cells present in neuronal- and glial-enriched mixed primary cell cultures, we performed preliminary studies of immunostaining of neurons, dopaminergic neurons, and astrocytes using anti-MAP2, anti-TH and anti-GFAP antibodies, respectively. In neuronal-enriched primary cell cultures, 89% of the cells were immunoreactive for the neuronal marker MAP2 and only 8.7% were astrocytes immunostained by anti-GFAP antibodies. Approximately half (47.3%) of the neurons were TH-positive dopaminergic neurons. In the glial-enriched cell cultures, 93.8% of the cells were GFAP-positive astrocytes. The proportions of these cells in the primary cultures were in agreement with those reported in a previous study using the same culture conditions (Iwata-Ichikawa et al., 1999).

Since several studies demonstrated that rotenone preferentially induced degeneration of dopaminergic neurons with shortening of the neurites (Nakao et al., 1997; Bywood and Johnson, 2003; Sawada et al., 2004), we determined the proper doses of rotenone to produce similar morphological changes in our cell culture system (Fig. 1). Neurons of the control group had long and thin neurites (Fig. 1A, B; arrows), while neurons treated with 5, 25 or 50 nM rotenone (Fig. 1C–H) showed progressive neurite retraction (Fig. 1; insets), which was especially observed in neurons treated with 25 and 50 nM rotenone (Fig. 1E–H; arrowheads). Moreover, rotenone treatment reduced the numbers of neurons stained by anti-MAP2 antibodies (Fig. 1A, C, E, G; green, J) and TH-immunoreactive neurons (Fig. 1B, D, F, H, J) in a dose-dependent manner. In contrast, the number of astrocytes immunostained by anti-GFAP antibodies was mildly affected by rotenone (Fig. 1A, C, E, G; red, J). Cell viability in neuronal- and glial-enriched mixed cultures was determined by Trypan Blue assay (Fig. 1I) or by direct counting of cells positive for MAP2, TH and GFAP (Fig. 1J). Although rotenone induced death of both neuronal and glial cells, TH-positive neurons were more sensitive to the toxic effects of 25 and 50 nM rotenone. Thus, rotenone at 25 and 50 nM caused both death of dopaminergic cells and neurite retraction.

Rotenone induces aggregation of centrosomal protein γ-tubulin

The distribution and concentration of the centrosomal protein γ-tubulin were examined in rotenone-treated mesencephalic neurons by immunostaining and Western blot analysis (Fig. 2). Normal neurons showed a diffuse signal of γ-tubulin protein, which was mainly concentrated in the base of the neurites (Fig. 2A; arrow). On the other hand, rotenone-treated neurons exhibited a perinuclear-spherical condensation of γ-tubulin immunofluorescence resembling protein aggregation (Fig. 2B–D). In few cells, the perinuclear condensation of γ-tubulin protein was elongated (data not shown). The diameter of these intense-perinuclear aggregates ranged from 2 to 4 μm, and the largest aggregates were observed in neurons treated with 25 and 50 nM rotenone (Fig. 2C, D). In several rotenone-treated neurons, the strongest signal of γ-tubulin was concentrated in the peripheral region of the aggregates resembling a halo (Fig. 2D; arrowhead). Curiously, neurons with perinuclear aggregates of γ-tubulin showed expansion of the neurite bases and neurite retraction (Fig. 2B–D), in contrast to the thin neurites observed in the control group (Fig. 2A).

Western blot analyses of the detergent-soluble and detergent-insoluble fractions of the cell lysates were conducted to estimate the concentration of γ-tubulin in both fractions. Western blotting (Fig. 2E, F) and densitometric analysis of the immunoblots (Fig. 2G, H) showed that γ-tubulin concentration diminished in a rotenone-dose dependent manner in the detergent-soluble fraction (Fig. 2E, G), but increased significantly in the detergent-insoluble fraction (Fig. 2F, H). These results indicate that rotenone induces aggregation of γ-tubulin protein in a dose dependent manner in primary cultures of mesencephalic neurons.

Rotenone induces important structural changes in centrosomes of TH-positive neurons and astrocytes

Since γ-tubulin is a centrosomal protein with a different distribution in neurons and glia (Leask et al., 1997), we studied the centrosomal structure in both mesencephalic-dopaminergic neurons and astrocytes (Fig. 3). Normal TH-positive neurons showed a diffuse signal of γ-tubulin rather than a localized staining of the centrosome (Fig. 3A–C) as described previously in post-mitotic neurons (Leask et al., 1997; McNaught et al., 2002b). Approximately 51.3%±6 (S.E.M.) of TH-positive rotenone-treated neurons (Fig. 3D–F) exhibited a single large stained focus of γ-tubulin protein mainly in the base of the neurites (Fig. 3E; arrow), which could represent enlarged centrosomes. Moreover, multiple centrosomes of different sizes were observed in several rotenone-treated neurons (Fig. 3E; inset). Both enlarged and multiple centrosomes were never seen in vehicle-treated neurons.

On the other hand, normal GFAP-positive astrocytes (Fig. 3G–I), showed a single signal for the centrosome (Fig. 3H). In contrast, 36.3%±5 (S.E.M.) of rotenone-treated astrocytes (Fig. 3J–L) exhibited multiple and disorganized centrosomes (Fig. 3K; arrowheads). A few astrocytes in the control group had two separate centrosomes possibly associated with the normal formation of bipolar spindles of mitosis. However, overduplicated and asymmetric centrosomes were never observed in normal astrocytes. Using antibodies against pericentrin, which is another protein usually identified in the pericentriolar ma-

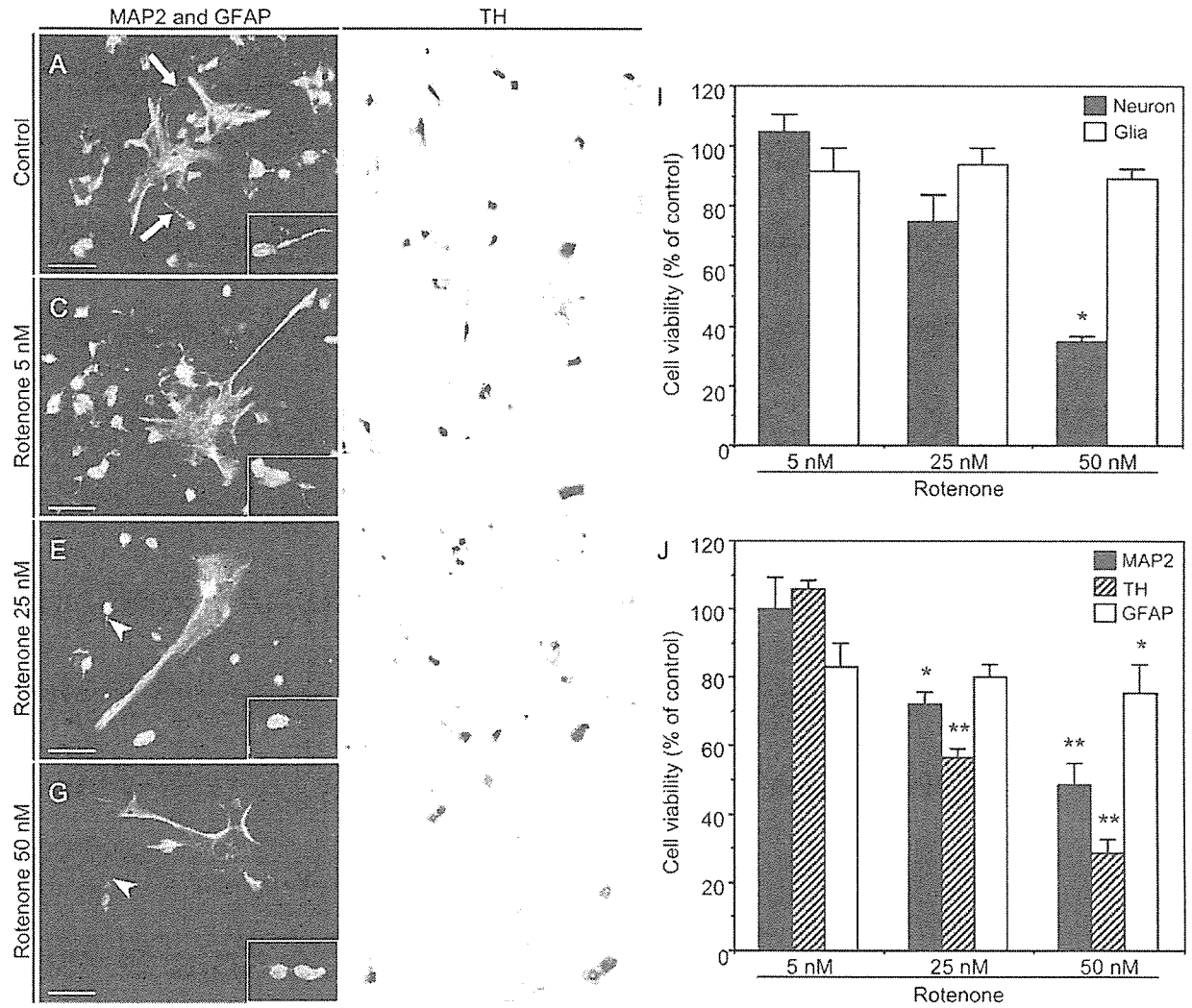

Fig. 1. Immunofluorescence staining of cultured mesencephalic cells (A–H), and quantification of cell viability in neuronal- and glial-enriched mixed cell cultures (I, J). Neuronal cell-enriched cultures were treated with vehicle (A, B) or different doses of rotenone (C–H) and then double immunostained with neuronal marker MAP2 (A, C, E, G; green) and astroglial marker GFAP (A, C, E, G; red). Immunohistochemical staining with anti-TH antibody and DAB detection was also performed to visualize dopaminergic neurons (B, D, F, H). Normal neurons showed long and thin neurites (arrows). Note the progressive neurite retraction in rotenone-treated neurons (arrowheads and insets). Cell viability of the neuronal- and glial-enriched mixed cultures was determined by Trypan Blue assay (I), and by direct count of cells positive for neuronal and glial markers (J). Note the significant cell loss of dopaminergic neurons treated with 25 and 50 nM rotenone (J). Values expressed in percentages represent means±S.E.M. of cell viability in four independent experiments. * $P<0.05$, ** $P<0.01$, compared with the respective control (vehicle only; one-way ANOVA followed by Dunnett's test). Each panel shows a representative picture of five views/chamber in four independent experiments. Scale bar=50 μm.

terial (Dictenberg et al., 1998), we found similar morphological changes in the centrosome of rotenone-treated cells (data not shown). These results indicate that rotenone treatment results in redistribution of γ-tubulin protein in dopaminergic neurons and astrocytes as well as disorganization of the centrosome.

Rotenone induces aggregation of α-synuclein protein in abnormal centrosomes

Since α-synuclein is a major component protein of the inclusion bodies in PD and other neurodegenerative diseases (Spillantini et al., 1997; Galvin et al., 2001) and because aggregates of α-synuclein are observed in neurons or glia (Wakabayashi et al., 2000), we determined the distribution of this protein and its relation to the centrosome in vehicle- and rotenone-treated neurons and astrocytes (Fig. 4). Vehicle-treated neurons showed diffuse signals of both γ-tubulin and α-synuclein proteins (Fig. 4A–C). While neurons treated with different doses of rotenone exhibited perinuclear aggregation of γ-tubulin, which was co-localized with α-synuclein (Fig. 4D–L). The majority of α-synuclein aggregates were observed in the base of the neurites (Fig. 4E; arrow). Neurons treated with higher doses of rotenone contained perinuclear protein aggregates of γ-tubulin and α-synuclein and showed evident neurite retraction (Fig. 4G–L).

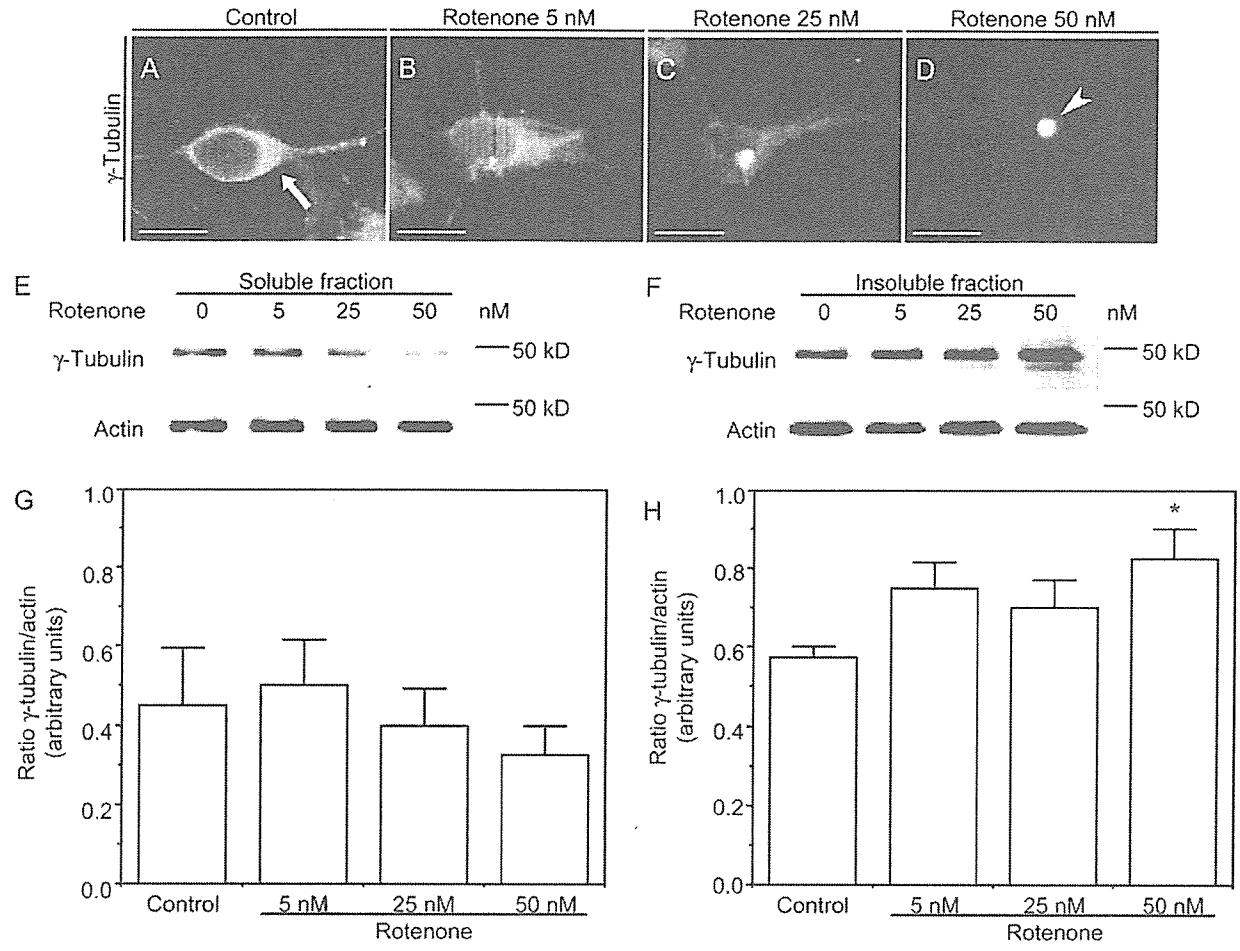

Fig. 2. Immunostaining of cultured mesencephalic neurons with anti-γ-tubulin antibody (A–D) and Western blot analyses of the γ-tubulin protein (E–H). Vehicle-treated neurons (A) showed diffuse positive signal for γ-tubulin mainly in the base of the neurites (arrow). Rotenone-treated neurons (B–D) exhibited intense perinuclear-spherical condensation of the γ-tubulin signal (arrowhead). Western blotting of the cell lysates (E, F) and densitometric analysis of the blots (G, H) showed reduced γ-tubulin concentration in the detergent-soluble fraction (E, G) and a significant increase of the protein in the detergent-insoluble fraction (F, H). Values expressed in arbitrary units represent means±S.E.M. of the ratio γ-tubulin/actin in four independent experiments. * $P<0.05$, compared with the control (one-way ANOVA followed by Dunnett's test). Each panel shows a representative picture of five views/chamber in four independent experiments. Scale bar=10 μm.

On the other hand, vehicle-treated astrocytes (Fig. 4M–O) showed a normal signal for the centrosome (Fig. 4M; arrowhead), which was not co-localized with any signal of the α-synuclein protein (Fig. 4N, O). On the other hand, multiple and asymmetric centrosomes found in rotenone-treated astrocytes were co-localized with perinuclear aggregates of α-synuclein (Fig. 4P–R). Although some neurons and glial cells containing abnormal centrosomes were negative for α-synuclein, every rotenone-treated neuron and glia with large aggregates of α-synuclein contained abnormal centrosomes. Thus, aggregation of α-synuclein by rotenone occurred only in neurons and glia cells that contained abnormal centrosomes.

Rotenone interrupts nucleation and stability of microtubules

One of the main functions of the centrosome and γ-tubulin protein is nucleation and organization of microtubules (Stearns et al., 1991; Draber and Draberova, 2003). The latter are polymers of repeating α- and β-tubulin subunits, which provide structural support for the axon and dendrites in neurons (Yu et al., 1993; Baas, 1996). In the next step, we studied whether the rotenone-induced structural changes of the centrosome affect the normal nucleation of microtubules and the normal morphology of neurites (Fig. 5). In normal neurons (Fig. 5A–C), microtubules were cramped into the neurites and were not attached to any centrosome-like nucleating structure (Fig. 5B). Microtubules in neurons are nucleated in the centrosome, but then are released and transported into the neurites (Yu et al., 1993; Baas, 1996). In vehicle-treated neurons, the β-tubulin signal was intensely co-localized with the γ-tubulin signal in the base of and along the neurites (Fig. 5C; arrows), in agreement with the report indicating that the brain γ-tubulin complex interacts with α-β tubulin polymers (Sulimenko et al., 2002). The intense signals of γ- and β-tubulins observed in

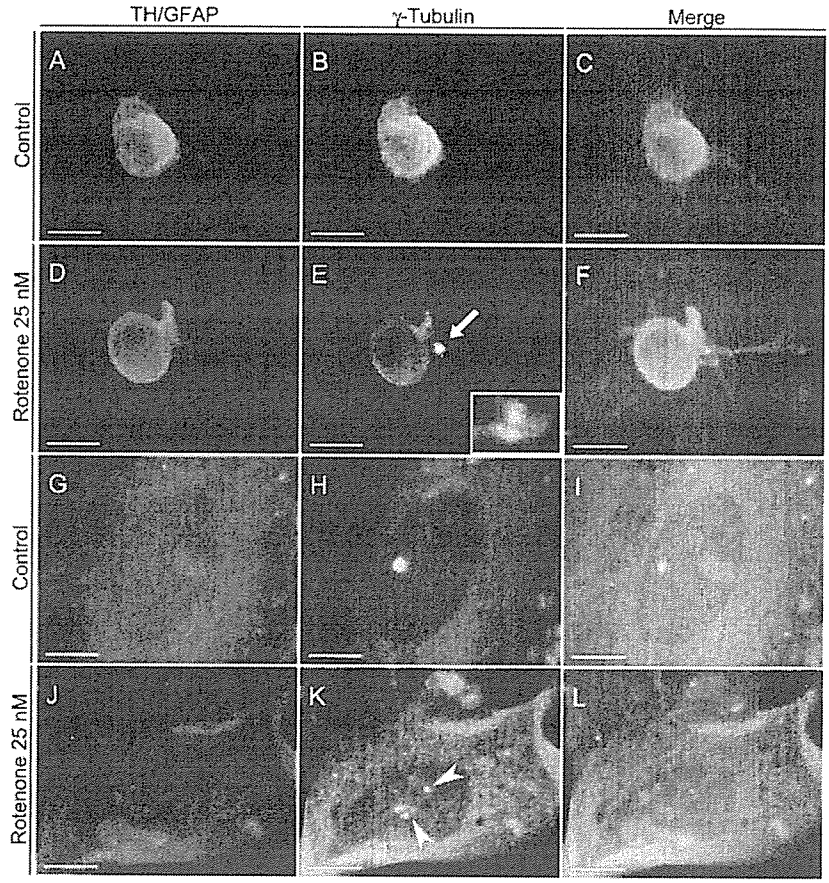

Fig. 3. Effects of rotenone on centrosome structure in mesencephalic dopaminergic neurons (A–F) and astrocytes (G–L). Cells were immunostained with anti-TH antibodies (red; A, D) and anti-GFAP antibody (red; G, J) as markers for dopaminergic neurons and astrocytes, respectively. Anti-γ-tubulin antibody was used to visualize the centrosome (green). The right column represents the corresponding merged images (C, F, I, L). Normal dopaminergic neurons showed a diffuse signal of the centrosomal protein γ-tubulin (A–C). Several dopaminergic neurons treated with rotenone (D–F) showed a large focus of γ-tubulin staining (arrow) or multiple centrosomes (inset). The majority of normal astrocytes (G–I) showed a single centrosome (H), while rotenone-treated astrocytes (J–L) contained multiple and disorganized centrosomes (arrowheads). Each panel shows a representative picture of five views/chamber in four independent experiments. Scale bar=10 μm.

normal neurites partially or completely disappeared following rotenone treatment (Fig. 5D–F). In addition, perinuclear and spherical aggregates of β-tubulin were observed next to the base of the neurites, which were co-localized with the γ-tubulin signal in enlarged centrosomes (Fig. 5D–F). The neurites of neuronal cells containing γ- and β-tubulin aggregates were generally shorter than those of normal neurons, and were also wide and tortuous.

To determine the distribution of the microtubules, we also performed immunostaining of astrocytes by using anti-β-tubulin antibodies. Normal astrocytes showed a complex network of long microtubules attached mainly to the centrosome (Fig. 5G–I). On the other hand, rotenone-treated astrocytes displayed a large amount of short and fragmented microtubules (Fig. 5J–L). Although most of the latter type were dispersed in the cytoplasm, others remained attached to the centrosome forming a dense condensation of the β-tubulin signal (Fig. 5L; arrow). Astrocytes containing multiple centrosomes exhibited an intricate conglomeration of microtubules in the perinuclear region (data not shown). These results indicate that rotenone markedly affects the nucleation and stability of microtubules, which results in structural changes in the cytoskeleton of both neurons and glia.

Rotenone causes disassembly of GA in neurons and astrocytes containing γ-tubulin aggregates and abnormal centrosomes

Since fragmentation of the GA has been linked to the pathogenesis of several representative neurodegenerative diseases, in which the aggregation of aberrant proteins has been also described (Stieber et al., 1996; Gonatas et al., 1998; Sakurai et al., 2000, 2002), we determined the distribution of GA in cells containing aggregates of γ-tubulin and abnormal centrosomes (Fig. 6). The majority of neurons in the vehicle treated group (Fig. 6A–C) contained one strong focus of GA signal in the base of the neurites (Fig. 6B; arrow), which was co-localized with the diffuse signal of the γ-tubulin (Fig. 6A, C). The distribution of both GA and centrosome signals is consistent with that previously reported in normal neurons (Zmuda and Rivas,

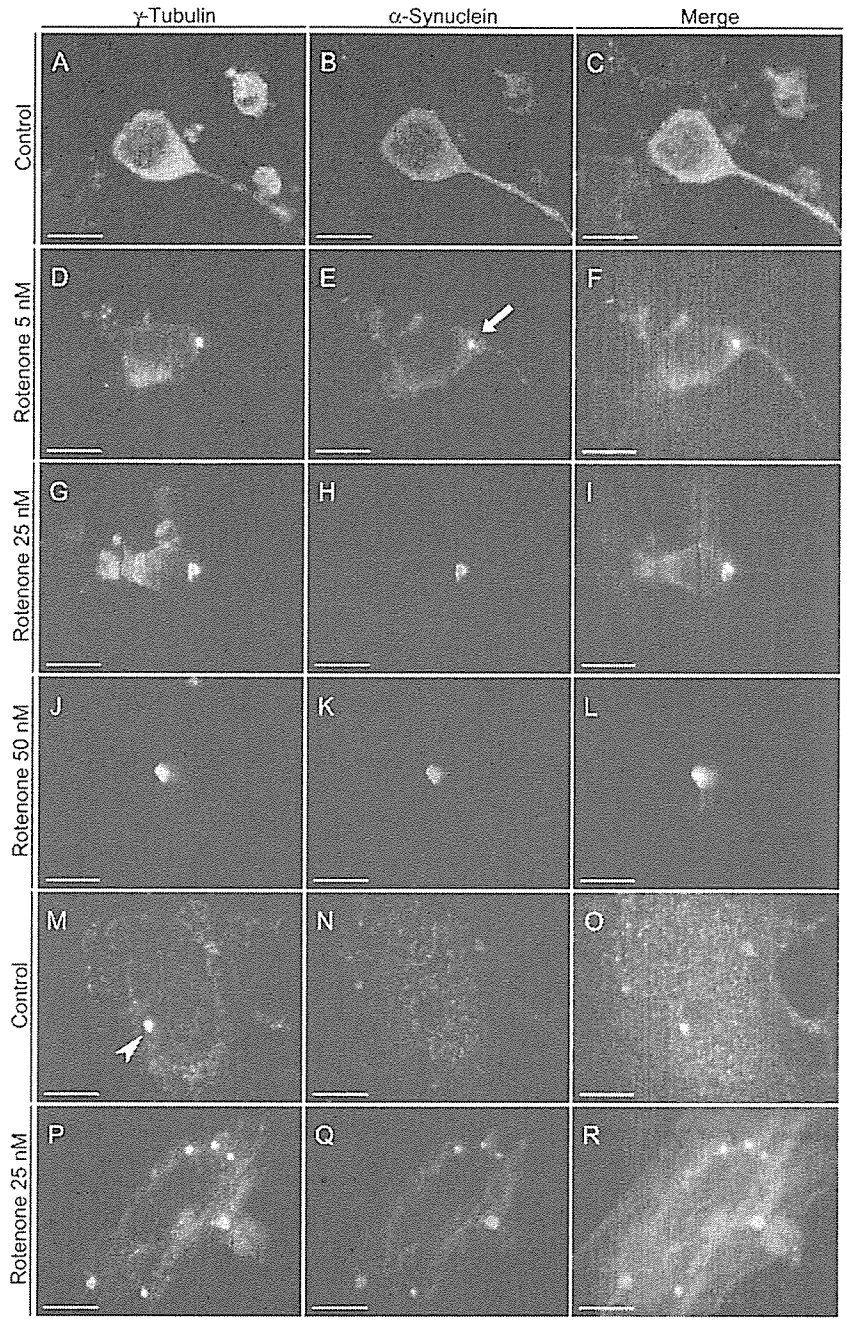

Fig. 4. Localization of γ-tubulin and α-synuclein proteins in mesencephalic dopaminergic neurons (A–L) and astrocytes (M–R). Double immunostaining for γ-tubulin (green) and α-synuclein proteins (red) was performed as described in Experimental Procedures. The right column represents the corresponding merged images (C, F, I, L, O, R). Vehicle-treated neurons showed diffuse signals of γ-tubulin and α-synuclein (A–C), while neurons treated with different doses of rotenone exhibited co-localization of γ-tubulin and α-synuclein in perinuclear aggregates (D–L). Note the intense signal of α-synuclein in the base of the neurite (arrow). Normal astrocytes (M–O) showed a clear signal for the centrosome (arrowhead), which were not co-localized with the α-synuclein signal (N, O). In contrast, multiple and perinuclear aggregates of both γ-tubulin and α-synuclein proteins were observed in rotenone-treated astrocytes (P–R). Each panel shows a representative picture of five views/chamber in four independent experiments. Scale bar=10 μm.

1998). On the other hand, rotenone-treated neurons with perinuclear aggregates of γ-tubulin and neurite retraction, exhibited a diffuse and weak signal of the GA (Fig. 6D–F). Neurons with destabilized microtubules also showed complete dispersion of the GA signal in the cytoplasm (data not shown).

The majority of normal astrocytes (Fig. 6G–I) showed a strong signal for GA located next to the centrosome (Fig. 6I;

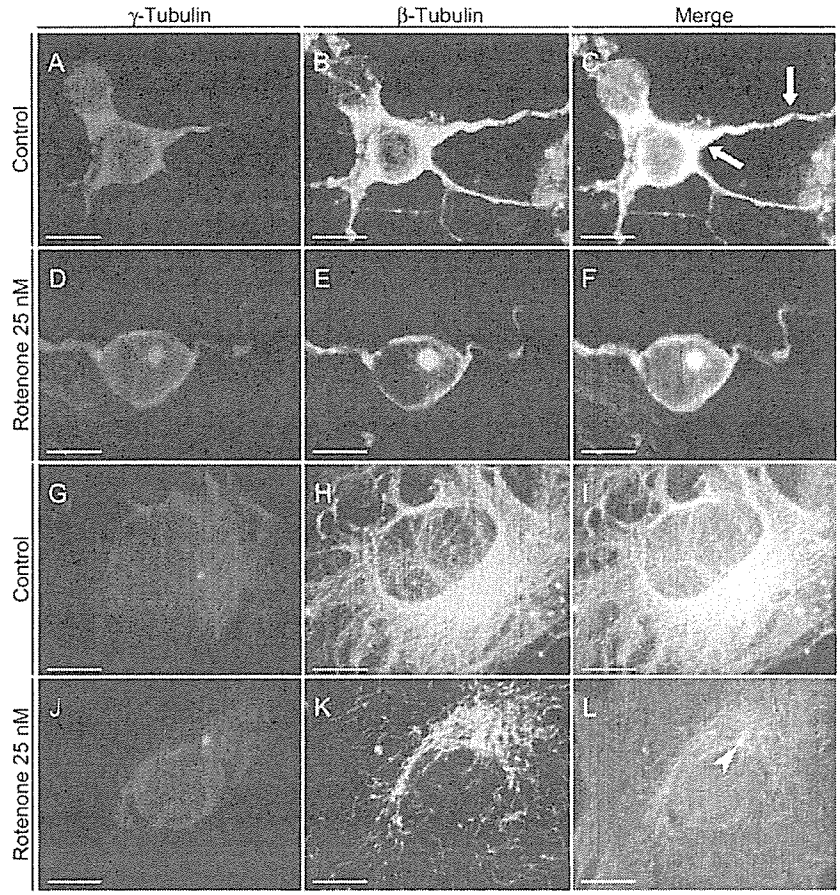

Fig. 5. Immunostaining of microtubules in primary cell culture of mesencephalic neurons (A–F) and astrocytes (G–L). Neuronal and astroglial cells were double immunostained with anti-γ-tubulin antibody to detect the centrosome (red) and with anti-β-tubulin antibody to detect the microtubules (green). The right column represents the corresponding merged images (C, F, I, L). Vehicle-treated neurons (A–C) showed β-tubulin signals in the base of and along the neurites, and co-localization with the γ-tubulin signals (arrows). These intense signals of γ-tubulin and β-tubulin in the neurites of normal neurons were lost in the rotenone-treated group, while large and perinuclear condensations of both proteins were observed next to the base of the neurites (D–F). Normal astrocytes showed a complex network of long microtubules mainly attached to the centrosome (G–I). In contrast, short and fragmented microtubules were observed in rotenone-treated astrocytes (J–L). Although many short microtubules were dispersed in the cytoplasm, others were still attached to the centrosome (arrowhead). Each panel shows a representative picture of five views/chamber in four independent experiments. Scale bar=10 μm.

arrowhead). In contrast, small fragments of GA were dispersed around the nucleus in rotenone-treated astrocytes containing multiple centrosomes (Fig. 6J–L). In order to quantify the effects of rotenone on the distribution of the GA, we counted the number of neurons with a single and strong focus of the γ-adaptin signal in the control group (Fig. 6M) and rotenone-treated groups (Fig. 6N–P) in four independent experiments. The normal distribution of GA significantly decreased in a dose-dependent manner in rotenone-treated groups (Fig. 6Q). These results indicate that rotenone induces a significant disassembly of the GA, coinciding with centrosomal disorganization and microtubule destabilization in both neurons and astrocytes.

Rotenone disrupts normal formation of mitotic spindles in astrocytes containing abnormal centrosomes

Since centrosomes and γ-tubulin are involved in the normal organization of mitotic spindles and consequently the balanced segregation of chromosomes in mitotic cells (Sunkel et al., 1995; Draber and Draberova, 2003), we examined the effect of rotenone on the conformation of mitotic spindles in astrocytes (Fig. 7). Normal astrocytes in interphase contained large and oval nuclei and showed a clear focal signal of the centrosome (Fig. 7A–C). In metaphase, the normal bipolar structure of the spindle was clearly visible with the chromosomes aligned at the equator of the cell. In early anaphase, the chromosomes begin to move toward the poles (Fig. 7D–F). In contrast, several rotenone-treated astrocytes (Fig. 7G–I) showed an aberrant and asymmetric nuclear division with multiple micronuclei (Fig. 7G; arrows), as well as abnormal multiplication of the centrosome (Fig. 7H; inset).

Normal neurons contained oval nuclei with diffuse and perinuclear γ-tubulin signal (Fig. 7J–L). Interestingly, rotenone treated-neurons (Fig. 7M–O) containing large γ-tubulin aggregates also exhibited nuclear fragmentation in different small portions (Fig. 7M; arrowhead). In several rote-

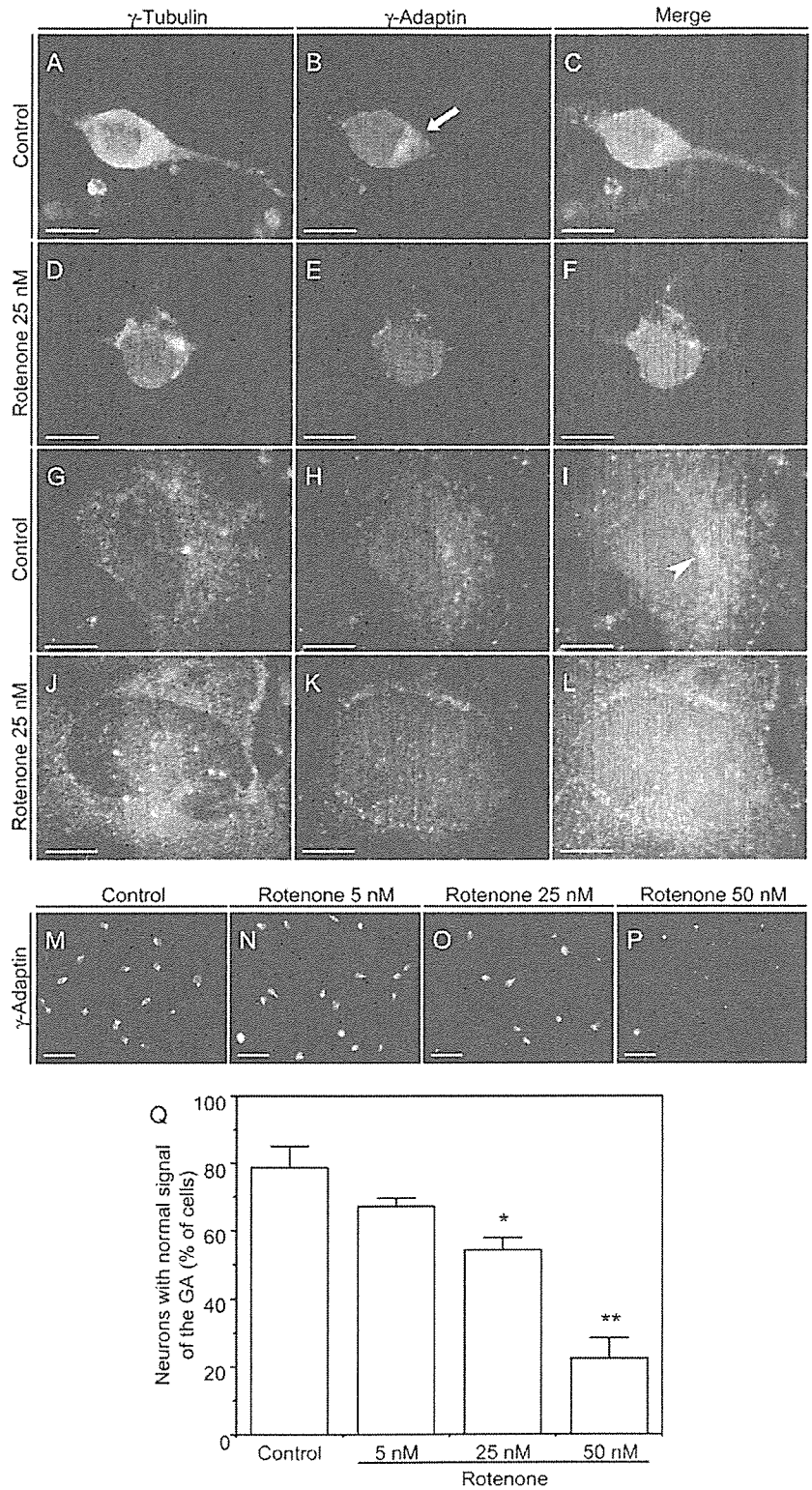

Fig. 6. Morphology of the GA in primary cultured neurons (A–F and M–P) and astrocytes (G–L). The centrosome and GA were immunostained with anti-γ-tubulin (green) and anti-γ-adaptin (red) antibodies, respectively. The right column represents the corresponding merged images (C, F, I, L). Neurons in the vehicle-treated group (A–C) showed a diffuse γ-tubulin signal (A) and one strong focus of GA located in the base of the neurite (arrow). While rotenone-treated neurons containing perinuclear aggregates of the γ-tubulin protein, displayed a diffuse and weak γ-adaptin-positive

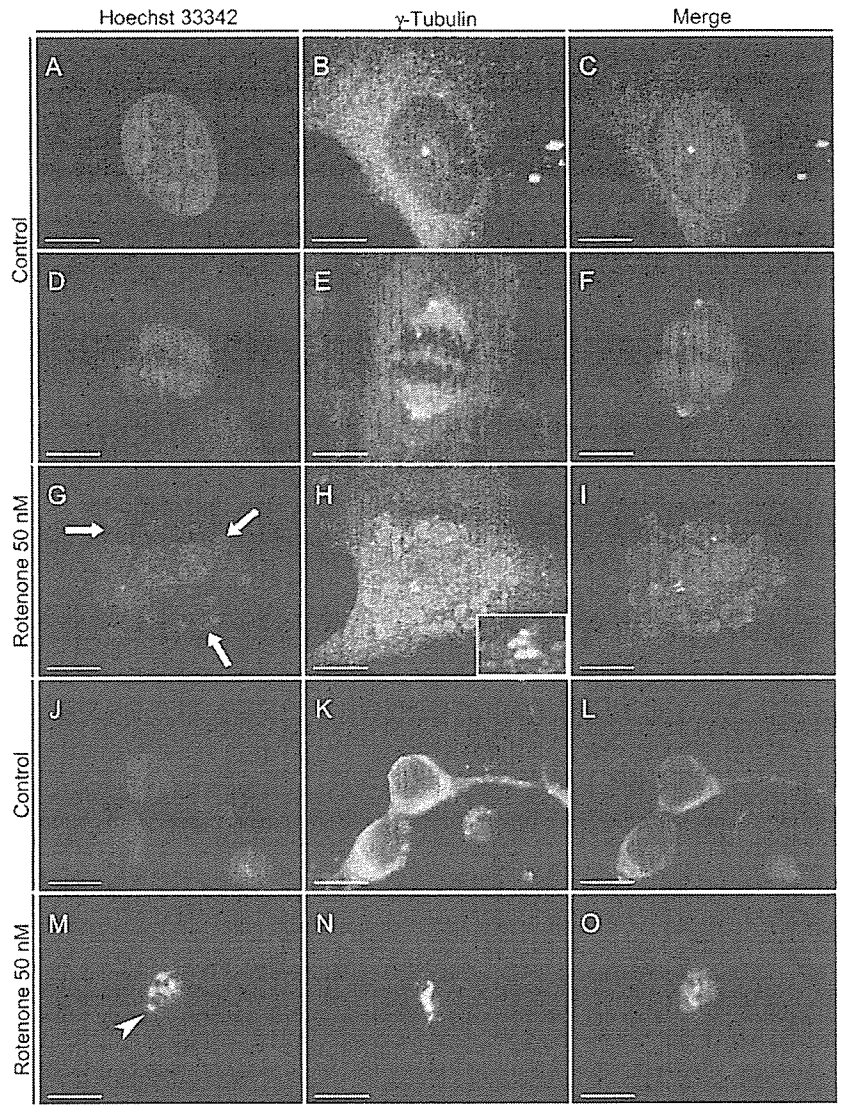

Fig. 7. Effects of rotenone on nuclear and centrosomal morphology in primary cultures of mesencephalic astrocytes (A–I) and neurons (J–O). Nuclei were stained by Hoechst 33342 dye (blue), and by anti-γ-tubulin antibody to visualize the centrosomes (green). The right column represents the corresponding merged images (C, F, I, L, O). Normal astrocytes in interphase (A–C) and early anaphase (D–F) contained a single centrosome and showed clear formation of mitotic spindles, respectively. Rotenone-treated astrocytes (G–I) exhibited an aberrant nuclear division with multiple micronucleus (arrows) and abnormal centrosomes (inset). Vehicle-treated neurons contained oval nuclei with diffuse γ-tubulin signal in the perinuclear region, especially in the base of the neurites (J–L). Rotenone-treated neurons (M–O) contained large and elongated γ-tubulin aggregates, displayed fragmentation of the nuclei into numerous small portions (arrowhead). Each panel shows a representative picture of five views/chamber in four independent experiments. Scale bar=10 μm.

none-treated astrocytes and neurons, large nuclei with vacuolization, as well as nuclear fragmentation by budding were also observed (data not shown). However, the majority of the cells in the rotenone-treated groups showed round and condensed nuclei. These findings suggest that rotenone induces abnormal mitotic spindles, which could interfere with the balanced segregation of the chromosomes in astrocytes. However, our results did not allow a

immunofluorescence of the GA (D–F). Normal astrocytes (G–I) exhibited a strong signal of the GA concentrated next to the centrosome (arrowhead). Multiple centrosomes and dispersion of the γ-adaptin signal were observed in astrocytes treated with rotenone (J–L). Note the normal immunofluorescence of the GA in different neurons in the control group (M) and the dose-dependent reduction of this signal in rotenone-treated neurons (N–P). Quantification of neurons with normal distribution of GA showed a significant reduction in the rotenone-treated groups (Q). Values expressed in percentage represent means±S.E.M. of cells with normal GA signal in four independent experiments. * $P<0.05$, ** $P<0.01$, compared with the control (one-way ANOVA followed by Dunnett's test). Each panel shows a representative picture of five views/chamber in four independent experiments. Scale bar=10 μm in panels (A–L), and in panels (M–P)=50 μm.

clear definition of the relation between centrosomal disorganization and changes in nuclear morphology in neurons, which are considered post-mitotic cells.

Long-term treatment of rats with rotenone induces hypokinesia, degeneration of dopaminergic neurons in the SN and appearance of pale and eosinophilic inclusion bodies

In order to study the distribution of γ-tubulin protein in the brain of Lewis rats treated with rotenone, we firstly confirmed the presence of parkinsonian features in our rotenone-treated rats (Fig. 8). Nine of the 20 rotenone-treated rats died within the first week of rotenone infusion. Only eight rats (40%) exhibited a reduction in spontaneous locomotor activity mainly during the first 2 weeks of treatment (Fig. 8A). Coronal sections of the SN (Fig. 8B, C) showed marked decrease of TH-immunoreactive neurons in rotenone-infused rats (Fig. 8C), in contrast to the abundant TH-positive signals in control rats (Fig. 8B). Rotenone also caused marked reduction of TH-positive dopaminergic terminals in the striatum (Fig. 8E) compared with the control (Fig. 8D). Neurons stained with hematoxylin and eosin in the SN of control rats displayed abundant cytoplasm and a fusiform shape (Fig. 8F; arrows). In contrast, rotenone treatment reduced the number of neurons as well as the cytoplasmic volume in these cells (Fig. 8G). Few of these atrophic neurons contained pale and eosinophilic inclusions (Fig. 8G; arrowhead). However, rotenone did not alter the size and shape of the nucleus of these neurons. Neurons in the striatal region did not show any inclusion body. These results indicate that long-term treatment of rats with rotenone results in the development of hypokinesia, degeneration of dopaminergic neurons in the SN and intracytoplasmic inclusion as described previously (Betarbet et al., 2000; Hoglinger et al., 2003; Sherer et al., 2003b).

Long-term treatment of rats with rotenone induces γ-tubulin aggregation and disassembly of GA in neurons of the SN

The aggregation of the γ-tubulin in dopaminergic neurons and astrocytes, as well as disassembly of the GA *in vivo*, was examined in SN sections of vehicle- and rotenone-treated rats by immunostaining with anti-TH, anti-GFAP, anti-γ-tubulin and anti-γ-adaptin antibodies (Fig. 9). The SN of control animals (Fig. 9A–C, G–I) contained numerous TH-positive neurons with abundant cytoplasm and fusiform shape (Fig. 9A). In addition, few GFAP-positive astrocytes were detected in control rats (Fig. 9G). The distribution of γ-tubulin was diffuse but weak and located in the perinuclear region in neurons of vehicle-treated rats (Fig. 9B, H). In contrast, rotenone-treated rats (Fig. 9D–F, J–L) displayed TH-positive neurons with shrunk cytoplasm (Fig. 9D). The number and size of GFAP-positive astrocytes were evidently increased in the SN of rotenone-treated rats (Fig. 9J). In these rotenone-treated rats, γ-tubulin immunoreactivity showed an unusual redistribution, with large amount of small and round aggregates (Fig. 9E, K; arrows). The majority of these aggregates were localized into the cytoplasm of TH-positive neurons (Fig. 9F). In addition, elongated forms of γ-tubulin aggregates were found in rotenone-treated rats (Fig. 9E, K; insets). These elongated aggregates were co-localized with TH-positive fibers (Fig. 9F; inset). Extracellular aggregates were also observed. Although multiple centrosomes were not found in astrocytes of rotenone-treated rats, the reactive astrogliosis observed in these animals was exclusively limited to the areas showing large number of γ-tubulin aggregates (Fig. 9L).

Finally, we examined the distribution of GA in neurons of the SN by immunohistochemistry using anti-γ-adaptin antibody (Fig. 9M–P). Normal neurons showed intense signal of GA in the perinuclear region mainly in one of the poles of the cell (Fig. 9M, N). In contrast, neurons of rotenone-treated animals showed diffuse and weak signal of the GA (Fig. 9O, P). Vacuolization of the cytoplasm was observed in several neurons with disassembly of the GA (Fig. 9P; arrowhead). The normal distribution of GA and the dispersion of γ-adaptin-positive signals observed in the SN of control and rotenone-treated rats, respectively, were similar to those observed in the primary cultured dopaminergic neurons shown in Fig. 6. These results indicate that rotenone induces aggregation of γ-tubulin protein and disassembly of the GA in the SN of Lewis rats. Both these two changes were also observed in our cell culture systems treated with rotenone.

DISCUSSION

There is increasing evidence at present in support of the hypothesis that inclusion bodies in neurodegenerative diseases could be formed through the aggresome-related process (Johnston et al., 1998; Kopito, 2000; Waelter et al., 2001; Lee et al., 2002; McNaught et al., 2002b; Corcoran et al., 2004). This hypothesis considers an interesting common final pathway in the aggregation of proteins in several neurodegenerative diseases. In the case of neurons as in many other cells, different factors can increase the number of misfolded or aberrant proteins such as DNA mutations or errors in RNA transcription, osmotic or oxidative stress, viral gene products, and inhibition of proteosome function (Johnston et al., 1998; Kopito, 2000; Olanow et al., 2004). During the aggresome-related process, all these abnormal proteins formed for different reasons should converge and aggregate into one specific organelle, the centrosome, where they interact with proteins of the proteolytic system, cytoskeleton elements, as well as centrosomal proteins (Olanow et al., 2004). Thus, different causes for protein aggregation in different neurodegenerative diseases could form inclusion bodies through one common mechanism. However, there is still discrepancy whether these protein–protein interactions in the centrosome protect the cell from potentially toxic misfolded proteins or contribute to the neuronal dysfunction and neuronal death (Johnston et al., 1998; Trojanowski et al., 1998; Kopito, 2000; Jellinger, 2003; Olanow et al., 2004; Tanaka et al., 2004).

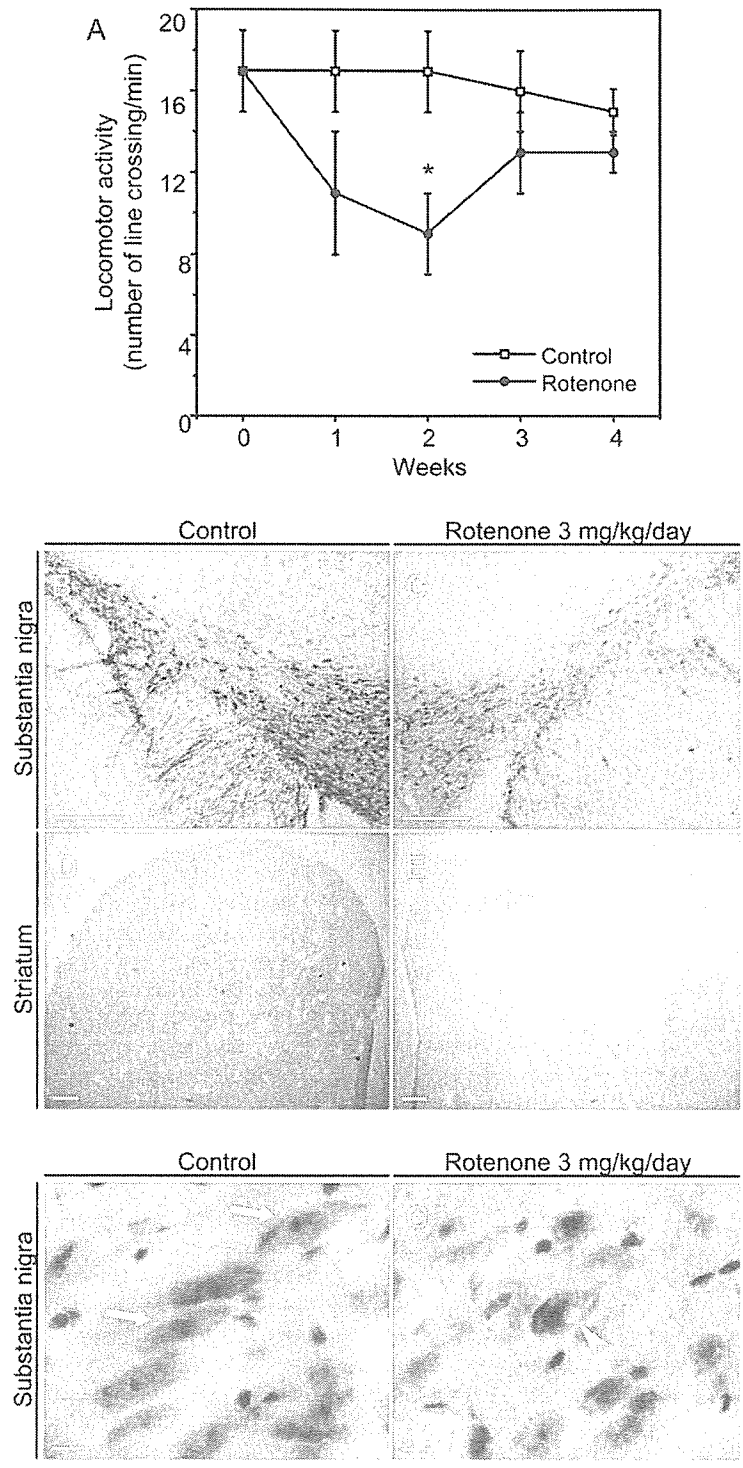

Fig. 8. Spontaneous locomotor activity (A), immunostaining of dopaminergic neurons using anti-TH antibody (B–E), and standard hematoxylin eosin staining of the SN (F, G) in Lewis rats infused with vehicle (B, D, F) or rotenone (3 mg/kg/day) for 4 weeks (C, E, G). Rotenone significantly reduced spontaneous locomotor activity ($P<0.01$, two-way ANOVA) but showed no time ($P=0.43$) or treatment–time interaction ($P=0.27$; A). The reduction in spontaneous locomotor activity by rotenone was observed mainly during the first 2 weeks of the treatment. Values represent the number of line crossing/minute and are expressed as mean±S.E.M. of spontaneous locomotor activity of eight Lewis rats. * $P<0.01$, compared with the respective time-matched untreated group (two-tailed Student's *t*-test). Coronal sections through the SN (B, C) and striatum (D, E) showed pronounced decreases in TH-immunoreactivity in rotenone-treated rats (C, E). Normal neurons in the SN of the control group displayed abundant cytoplasm (F) and a fusiform shape (arrows). Few atrophic neurons in the SN of rotenone-treated rats (G) displayed pale and eosinophilic inclusions in the cytoplasm (arrowhead). Each panel shows a representative picture of four independent experiments. Scale bars=250 μm in panels (B–E), and in panels (F, G)=10 μm.

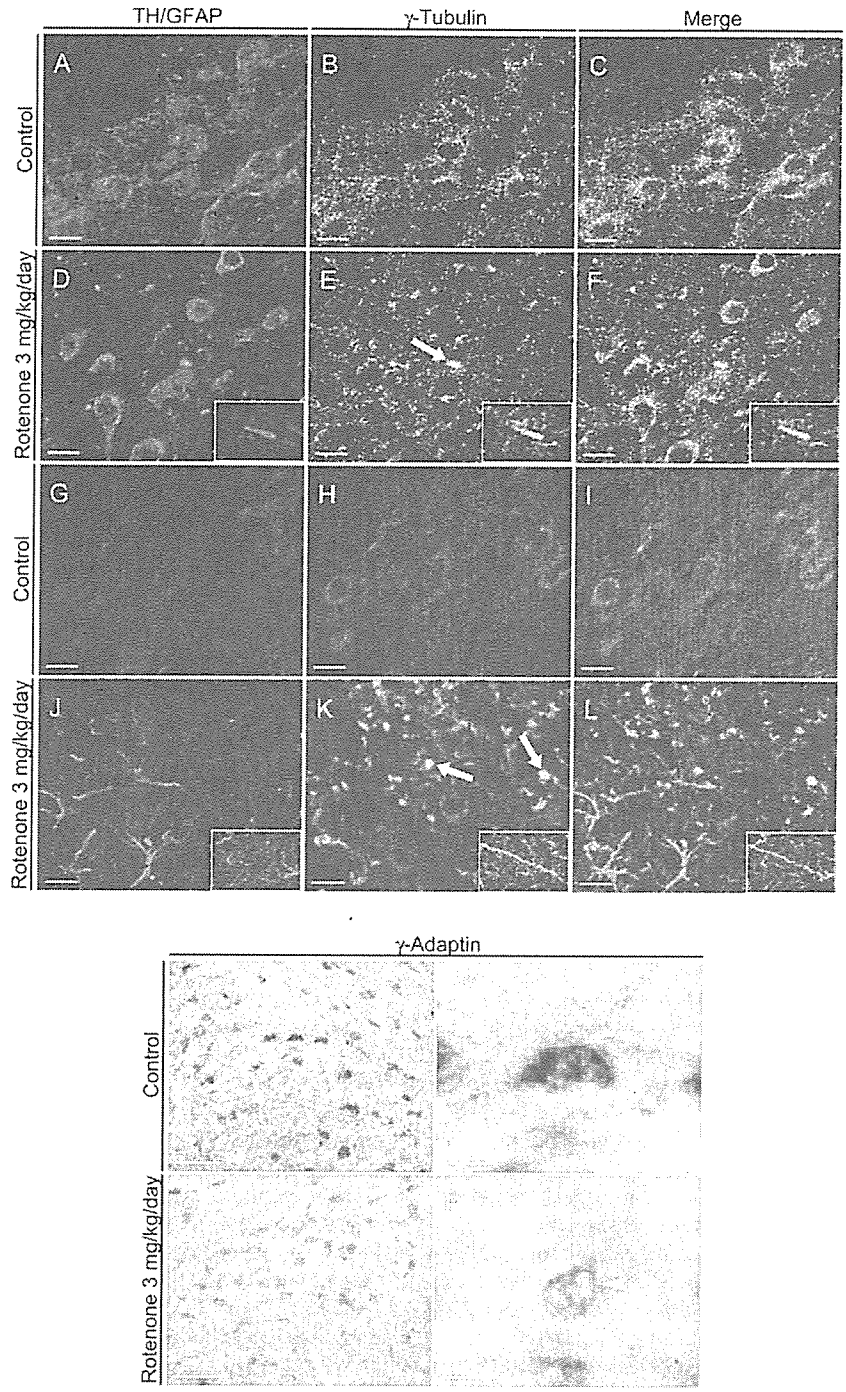

Fig. 9. Effects of rotenone on the distribution of γ-tubulin protein (A–L) and morphology of GA (M–P) in the SN of Lewis rats treated with vehicle (A–C, G–I, M, N) or rotenone (3 mg/kg/day) for 4 weeks (D–F, J–L, O, P). SN sections were immunostained with anti-TH (red; A, D), anti-GFAP (red; G, J), anti-γ-tubulin (green) and anti-γ-adaptin antibodies. The right column represents the corresponding merged images (C, F, I, L). Normal TH-positive neurons in the SN showed a diffuse signal of γ-tubulin in the perinuclear region (A–C). Coronal sections through the SN of treated rats (D–F) exhibited γ-tubulin aggregates (E; arrow and inset). Rotenone-treated rats (J–L) showed reactive astrocytosis in the same area where multiple γ-tubulin aggregates and dystrophic fibers were present (J–L; arrows and insets). In contrast, control animals showed few GFAP-positive astrocytes and diffuse signal of γ-tubulin in the SN (G–I). Normal neurons in the SN displayed an intense perinuclear signal of the GA (M, N). In contrast, diffuse and weak signals of γ-adaptin were identified in neurons of rotenone-treated rats (O, P). Moreover, vacuolization of the cytoplasm was observed in neurons showing GA disassembly (arrowhead). Each panel shows a representative picture of four independent experiments. Scale bars=10 μm in panels (A–L), in panels (M, O)=50 μm, and in panels (N, P)=10 μm.

In this study, we demonstrated that the insecticide rotenone induces perinuclear aggregation of the centrosomal protein γ-tubulin, as well as disorganization and dysfunction of the centrosome. Treatment of mesencephalic neuronal-enriched cell cultures with 5, 25 and 50 nM rotenone resulted in the formation of intracytoplasmic aggregates of γ-tubulin protein of different sizes and usually with a round shape. The lowest dose of rotenone induced perinuclear condensation of γ-tubulin in small aggregates. In contrast, cells treated with the highest doses of rotenone showed large aggregates with a complex distribution of γ-tubulin, which sometimes showed a halo pattern (Fig. 2). It has been reported that γ-tubulin or α-synuclein proteins are mainly concentrated in the peripheral halo of LBs of PD patients (McNaught et al., 2002b; Olanow et al., 2004). On the other hand, we demonstrated that rotenone resulted in a significant increase in the concentration of insoluble γ-tubulin, while the amount of this protein in the detergent-soluble fraction decreased in a dose-dependent manner (Fig. 2). Thus, not only the normal distribution but also the configuration of γ-tubulin protein itself seems to change radically to produce complex proteinaceous aggregates during the formation of inclusion bodies following rotenone treatment. Western blot analysis of brain samples of PD patients has shown also an increment in the concentration of γ-tubulin protein (McNaught et al., 2002b), suggesting the important role of this protein in the formation of LBs.

Rotenone produced marked morphological changes in the centrosome in cultured neurons and glia (Fig. 3). In rotenone-treated neurons, aggregation of γ-tubulin was associated with enlargement of centrosomes mainly located in the base of the neurites. Several rotenone-treated neurons showed two or three multiple centrosomes of different sizes. Furthermore, rotenone-treated astrocytes exhibited multiple centrosomes dispersed around the nucleus or concentrated in the middle of the cell (Fig. 3). α-Synuclein aggregates were localized exclusively in these abnormal centrosomes in both neurons and glia (Fig. 4). In contrast, not all γ-tubulin abnormal aggregates were α-synuclein immunoreactive. These observations suggest first that aggregation of γ-tubulin and α-synuclein, as well as centrosomal disorganization, are not a specific feature of neuronal cells, and second that α-synuclein aggregates are important but not essential for the formation of centrosomal proteinaceous aggregates. Indeed, abnormal aggregation of α-synuclein has been also observed into astrocytes and oligodendrocytes in brain samples of multiple system atrophy (MSA), DLB and PD patients (Gai et al., 1999; Wakabayashi et al., 2000). Moreover, it has been reported that several small perinuclear aggregates of different ubiquitinated proteins did not co-localize with α-synuclein protein in the SN of PD patients (McNaught et al., 2002b). On the other hand, we observed a redistribution of γ-tubulin in the SN of rotenone-treated rats (Fig. 9). The γ-tubulin aggregates were observed either in the cytoplasm of TH-neurons or TH-positive dystrophic fibers. However, several aggregates were not found in dopaminergic neurons, but rather seemed to be in the extracellular space. Interestingly, astrogliosis was noted exclusively in the same nigral areas of rotenone-treated rats where the γ-tubulin aggregates appeared (Fig. 9). Dystrophic fibers, extracellular inclusion bodies and reactive astrogliosis are also histopathological features of PD (Yamada et al., 1991; Braak et al., 1995; Sherer et al., 2003a). Thus, γ-tubulin protein may be involved not only in the formation of intracellular inclusion bodies, but also in the abnormal aggregation of proteins in neurites and extracellular space.

Although abnormal aggregation of both γ-tubulin and α-synuclein proteins was observed in both neurons and astrocytes (Fig. 4), cell viability was significantly reduced in rotenone-treated dopaminergic neurons and to a lesser extent in rotenone-treated astrocytes (Fig. 1). Moreover, the majority of γ-tubulin aggregates in neuronal cells were observed in TH-positive dopaminergic neurons (Fig. 3), while a few non-dopaminergic neurons contained these aggregates. It is still controversial whether the dopaminergic neurons are vulnerable to the toxic effects of rotenone, and whether they are predisposed to the formation of inclusion bodies. Primary mesencephalic cultures treated with low doses of rotenone showed a selective death of dopaminergic neurons, which was blocked by α-methyl-*p*-tyrosine, an inhibitor of dopamine synthesis (Sakka et al., 2003). The aggregation of γ-tubulin and α-synuclein specifically in dopaminergic neurons was previously reported in primary mesencephalic cultured cells treated with lactacystin or canavanine to inhibit proteasome function or to generate misfolded proteins, respectively (McNaught et al., 2002b). In addition, the formation of inclusion bodies in PC12 cells induced by lactacystin was prevented by reserpine, a dopamine-depleting agent (Fornai et al., 2003). Thus, endogenous dopamine could enhance the formation of inclusion bodies in dopaminergic neurons and neuronal cell death after rotenone treatment. However, the absence of endogenous dopamine in neurons could not be a limitation for the formation of LBs, because LBs are also observed in various non-dopaminergic neurons in different regions of the central nervous system of PD patients (Forno, 1996).

In addition to the morphological changes of the centrosome, rotenone also modulated the normal function of this organelle. We found that the β-tubulin signal, a marker for microtubules, disappeared partially or completely in neurites of several rotenone-treated neurons (Fig. 5). These neurons with microtubule destabilization showed perinuclear aggregates of β-tubulin protein, which were co-localized with γ-tubulin in enlarged centrosomes (Fig. 5). Moreover, the neurites of these cells showed significant or marked structural changes. Accumulation of tubulins and other cytoskeleton proteins has been reported in LBs of DLB patients, in whom the axonal transport is presumably blocked (Iseki et al., 2000). It has been reported that centrosomal inhibition by γ-tubulin antibodies either compromised or completely abolished axonal growth in primary cultured neurons (Ahmad et al., 1994). In addition, the proteasome inhibitor lactacystin can also induce the aggregation of α-synuclein in the centrosome, as well as neurite retraction in dopaminergic and non-dopaminergic cultured neurons (McNaught et al., 2002a,b; Laser et al.,

2003). Therefore, the structural modifications of neurites observed in rotenone-treated neurons could be a direct consequence of microtubule destabilization due to centrosomal dysfunction. On the other hand, astrocytes treated with rotenone also showed a clear microtubule destabilization and β-tubulin aggregates (Fig. 5). The glial inclusion bodies of MSA patients also show the presence of β-tubulin proteins (Gai et al., 1999). Thus, disturbances of the cytoskeleton could be a crucial effect of rotenone toxicity in promoting neuronal and astroglial cell damage. Indeed, disturbances of the cytoskeleton and disruption of neuronal transport are considered to be related to the pathogenesis of several neurodegenerative diseases including PD (D'Andrea et al., 2001; Crosby, 2003).

Recently, we reported that rotenone induced disassembly of the GA in the neuroblastoma B65 cell line in the early stages of apoptosis before activation of caspase-3, and suggested that aggregated proteins could be a possible cause of the GA disassembly in B65 rotenone-treated cells (Diaz-Corrales et al., 2004). Using primary cultured cells in the present study, we showed disassembly of the GA in rotenone-treated neurons and astrocytes (Fig. 6), as well as in the SN of Lewis rats chronically treated with rotenone (Fig. 9). Moreover, we demonstrated that disassembly of the GA occurred in cells containing protein aggregates and abnormal centrosomes. It has been reported that fragmentation of the GA observed in COS-7 cell infected with adenoviral vector carrying α-synuclein cDNA is the consequence of α-synuclein aggregation (Gosavi et al., 2002). In addition, it has been demonstrated that microtubule-depolymerizing drugs can induce fragmentation of the GA in neuronal and non-neuronal cells (Iida and Shibata, 1991; Lowenstein et al., 1994). Thus, we suggest that large centrosomal-protein aggregates and the consequent centrosomal dysfunction and microtubule destabilization could be the cause for disassembly of the GA observed in primary cell cultures and Lewis rats treated with rotenone. In the present study, we used an antibody against γ-adaptin protein, a component of the clathrin-coated vesicles of the GA (Robinson, 1990). Anti-γ-adaptin antibody can be used as a marker for the structure and function of the *trans*-Golgi network (Wagner et al., 1994). Therefore, redistribution of γ-adaptin signals observed in rotenone-treated cells represents or shows the structural changes in the morphology of GA, as well as alteration in the normal function of this organelle. The GA is a major cytoplasmic organelle involved in the intracellular trafficking of secretory and lysosomal proteins, and this organelle, together with the centrosome and microtubules, is essential for the structural formation and outgrowth of neurites (Rogalski and Singer, 1984; Letourneau and Wire, 1995; Zmuda and Rivas, 1998). Therefore, any dysfunction of these organelles should inevitably interfere with axonal transport and consequently with normal synaptic transmission.

In addition to microtubule nucleation, another important function of the centrosome and γ-tubulin is the formation of mitotic spindles (Draber and Draberova, 2003). In normal mitotic cells, the centrosome duplicates once per each cell cycle, then the pair of centrosomes is positioned in the opposite sides of the nucleus to establish the mitotic spindles (Sato et al., 2000). In our study, several rotenone-treated astrocytes contained multiple centrosomes and showed aberrant–asymmetric nuclear division with a large amount of micronuclei, instead of the normal formation of the mitotic spindle and balanced chromosome segregation observed in vehicle-treated astrocytes (Fig. 7). Multipolar spindles and mitotic arrest have been described previously in Chinese hamster cells treated with rotenone (Brinkley et al., 1974; Matsumoto and Ohta, 1993). Although the real cause of these observations has not yet been clarified, there is evidence to suggest that rotenone binds directly to the tubulin proteins (Brinkley et al., 1974; Marshall and Himes, 1978). It has been reported that mutation in the γ-tubulin gene induces destabilization of microtubules, abnormal centrosomes and mitotic arrest in *Drosophila* neuroblasts (Sunkel et al., 1995). On the other hand, experimental models of HD, an autosomal dominant polyglutamine disorder caused by mutation of the IT-15 gene encoding the huntingtin protein, have also shown that the abnormal huntingtin is co-localized with γ-tubulin in the centrosome (Waelter et al., 2001; Hoffner et al., 2002). Moreover, neurons expressing the mutant huntingtin showed progressive microtubule destabilization and neurite retraction after accumulation of the mutant huntingtin protein (Trushina et al., 2003). Interestingly, fibroblast cultures from HD patients have also shown centrosome disorganization, abnormal nuclear fragmentation and high frequency of micronuclei (Sathasivam et al., 2001). These observations are similar to the changes seen in rotenone-treated astrocytes in the present study. Considered together, it is possible that the formation of multipolar mitotic spindles in rotenone-treated astrocytes is due to changes in the configuration of γ-tubulin as a result of abnormal protein–protein interaction in the centrosome or represents the direct effect of the insecticide on tubulin proteins.

Although mitotic spindles and cell division are not present in normal post-mitotic neurons, abnormal expression of several cell cycle-regulatory proteins has been described in neurons of certain neurodegenerative diseases including PD, suggesting that aberrant mitotic activation of neurons could play a important role in the neurodegenerative process (Nagy et al., 1998; Husseman et al., 2000; Yang et al., 2001; Lee et al., 2003). Neurons in the SN pars compacta of rats treated with 6-hydroxydopamine overexpress Cdc2, a cell cycle-regulating protein kinase localized in the centrosome (Pockwinse et al., 1997; El-Khodor et al., 2003). Furthermore, mice treated with 1-methyl-4-phenyl-1,2,3,6-tetrahydropyridine (MPTP) also overexpressed cyclin-dependent kinase (Cdk) 2, which regulates the normal duplication of the centrosome in mammalian cells (Lacey et al., 1999; Smith et al., 2003). Overexpression of Cdk2 induces multiple centrosomes and chromosome instability in neoplastic cell lines (Kawamura et al., 2004), similar to the effects of rotenone in cultured astrocytes. In addition, LBs of PD patients are immunoreactive to Cdk5 and cyclin B (Brion and Couck, 1995; Lee et al., 2003). These two cell cycle-regulating proteins are related directly to axonal outgrowth and disassembly of the GA,

respectively (Draviam et al., 2001; Paglini et al., 2001). Interestingly, inhibition of both Cdk2 and Cdk5 proteins provides protection of dopaminergic neurons against MPTP (Smith et al., 2003). Based on the results of the above studies and the present findings, it is essential to clarify whether the nuclear fragmentation observed in neurons with centrosomal disorganization corresponds to the last step of the apoptotic process, or whether it represents abnormal chromosome segregation due to aberrant mitotic activation. In addition, further studies are required to establish the relationship between centrosomal disorganization, microtubule destabilization, GA disassembly and abnormal expression of cell cycle-regulating proteins in rotenone-treated cells and animal models of neurodegenerative diseases.

We postulate that rotenone could induce protein aggregation in neuronal cells through various mechanisms previously reported such as complex I inhibition, increased free radical generation or inhibition of the ubiquitin–proteasome system. However, centrosomal dysfunction could also play a key role in rotenone-induced neurotoxicity. The aberrant proteins induced by rotenone treatment could accumulate in the centrosome through a retrograde transport along microtubules, as described in the aggresome-related process. If the amount of aberrant proteins accumulated in the centrosome is limited, the ubiquitin–proteasome system or autophagic mechanisms should be capable of degrading and clearing these protein aggregates. Thus, accumulation of small amounts of unwanted proteins in the centrosome should protect the cell from potentially toxic proteins. Indeed, we observed that dopaminergic neurons treated with a low dose (5 nM) of rotenone developed small perinuclear aggregates of γ-tubulin and α-synuclein proteins, but the low dose did not influence cell viability or neurite structures. These results suggest that the effect of low-dose rotenone on the production of unwanted proteins did not overwhelm the capacity of degradation or clearance systems of unwanted proteins accumulated in the centrosome. This was in contrast to the formation of large and complex centrosomal aggregates induced by higher doses of rotenone (25 and 50 nM), which was associated with neurite retraction and neuronal cell death. These enlarged-protein aggregates in the centrosome may inevitably change the configuration of γ-tubulin and other centrosomal proteins. In conclusion, our results showed that disorganization and severe dysfunction of the centrosome induced by rotenone may cause microtubule destabilization, neurite retraction, disassembly of the GA and the collapse of neuronal cells. Our results may be potentially useful for the design of new drugs that prevent disorganization of the centrosome and destabilization of microtubules in neurodegenerative diseases.

Acknowledgments—This work was supported in part by Grants-in-Aid for Scientific Research (C) and for Encouragement of Young Scientists (B) from the Japanese Ministry of Education, Culture, Sports, Science, and Technology, and by Grants-in-Aid for Research on Psychiatric and Neurological Diseases and Mental Health, and Comprehensive Research on Aging and Health from the Japanese Ministry of Health, Labor and Welfare. We thank Mr. Kazunari Onishi for the excellent technical assistance.

REFERENCES

Ahmad FJ, Joshi HC, Centonze VE, Baas PW (1994) Inhibition of microtubule nucleation at the neuronal centrosome compromises axon growth. Neuron 12:271–280.

Asanuma M, Nishibayashi S, Kondo Y, Iwata E, Tsuda M, Ogawa N (1995) Effects of single cyclosporin A pretreatment on pentylenetetrazol-induced convulsion and on TRE-binding activity in the rat brain. Brain Res Mol Brain Res 33:29–36.

Baas PW (1996) The neuronal centrosome as a generator of microtubules for the axon. Curr Top Dev Biol 33:281–298.

Betarbet R, Sherer TB, MacKenzie G, Garcia-Osuna M, Panov AV, Greenamyre JT (2000) Chronic systemic pesticide exposure reproduces features of Parkinson's disease. Nat Neurosci 3:1301–1306.

Braak H, Braak E, Yilmazer D, Schultz C, de Vos RA, Jansen EN (1995) Nigral and extranigral pathology in Parkinson's disease. J Neural Transm (Suppl) 46:15–31.

Brinkley BR, Barham SS, Barranco SC, Fuller GM (1974) Rotenone inhibition of spindle microtubule assembly in mammalian cells. Exp Cell Res 85:41–46.

Brion JP, Couck AM (1995) Cortical and brainstem-type Lewy bodies are immunoreactive for the cyclin-dependent kinase 5. Am J Pathol 147:1465–1476.

Bywood PT, Johnson SM (2003) Mitochondrial complex inhibitors preferentially damage substantia nigra dopamine neurons in rat brain slices. Exp Neurol 179:47–59.

Corcoran LJ, Mitchison TJ, Liu Q (2004) A novel action of histone deacetylase inhibitors in a protein aggresome disease model. Curr Biol 14:488–492.

Crosby AH (2003) Disruption of cellular transport: a common cause of neurodegeneration? Lancet Neurol 2:311–316.

D'Andrea MR, Ilyin S, Plata-Salaman CR (2001) Abnormal patterns of microtubule-associated protein-2 (MAP-2) immunolabeling in neuronal nuclei and Lewy bodies in Parkinson's disease substantia nigra brain tissues. Neurosci Lett 306:137–140.

Diaz-Corrales FJ, Asanuma M, Miyazaki I, Ogawa N (2004) Rotenone induces disassembly of the Golgi apparatus in the rat dopaminergic neuroblastoma B65 cell line. Neurosci Lett 354:59–63.

Dictenberg JB, Zimmerman W, Sparks CA, Young A, Vidair C, Zheng Y, Carrington W, Fay FS, Doxsey SJ (1998) Pericentrin and gamma-tubulin form a protein complex and are organized into a novel lattice at the centrosome. J Cell Biol 141:163–174.

Draber P, Draberova E (2003) Gamma-tubulins and their functions. Tsitol Genet 37:3–10.

Draviam VM, Orrechia S, Lowe M, Pardi R, Pines J (2001) The localization of human cyclins B1 and B2 determines CDK1 substrate specificity and neither enzyme requires MEK to disassemble the Golgi apparatus. J Cell Biol 152:945–958.

El-Khodor BF, Oo TF, Kholodilov N, Burke RE (2003) Ectopic expression of cell cycle markers in models of induced programmed cell death in dopamine neurons of the rat substantia nigra pars compacta. Exp Neurol 179:17–27.

Fornai F, Lenzi P, Gesi M, Ferrucci M, Lazzeri G, Busceti CL, Ruffoli R, Soldani P, Ruggieri S, Alessandri MG, Paparelli A (2003) Fine structure and biochemical mechanisms underlying nigrostriatal inclusions and cell death after proteasome inhibition. J Neurosci 23:8955–8966.

Forno LS (1996) Neuropathology of Parkinson's disease. J Neuropathol Exp Neurol 55:259–272.

Fukami H, Nakajima M (1971) Rotenone and the rotenoids. In: Naturally occurring insecticides (Jacobson M, Crosby DG, eds), pp 71–97. New York: Marcel Dekker.

Fuller SD, Gowen BE, Reinsch S, Sawyer A, Buendia B, Wepf R, Karsenti E (1995) The core of the mammalian centriole contains gamma-tubulin. Curr Biol 5:1384–1393.

Gai WP, Blessing WW, Blumbergs PC (1995) Ubiquitin-positive degenerating neurites in the brainstem in Parkinson's disease. Brain 118:1447–1459.

Gai WP, Power JH, Blumbergs PC, Culvenor JG, Jensen PH (1999) Alpha-synuclein immunoisolation of glial inclusions from multiple system atrophy brain tissue reveals multiprotein components. J Neurochem 73:2093–2100.

Galvin JE, Lee VM, Trojanowski JQ (2001) Synucleinopathies: clinical and pathological implications. Arch Neurol 58:186–190.

Gonatas NK, Gonatas JO, Stieber A (1998) The involvement of the Golgi apparatus in the pathogenesis of amyotrophic lateral sclerosis, Alzheimer's disease, and ricin intoxication. Histochem Cell Biol 109:591–600.

Gosavi N, Lee HJ, Lee JS, Patel S, Lee SJ (2002) Golgi fragmentation occurs in the cells with prefibrillar alpha-synuclein aggregates and precedes the formation of fibrillar inclusion. J Biol Chem 277: 48984–48992.

Hoffner G, Kahlem P, Djian P (2002) Perinuclear localization of huntingtin as a consequence of its binding to microtubules through an interaction with beta-tubulin: relevance to Huntington's disease. J Cell Sci 115:941–948.

Hoglinger GU, Feger J, Prigent A, Michel PP, Parain K, Champy P, Ruberg M, Oertel WH, Hirsch EC (2003) Chronic systemic complex I inhibition induces a hypokinetic multisystem degeneration in rats. J Neurochem 84:491–502.

Husseman JW, Nochlin D, Vincent I (2000) Mitotic activation: a convergent mechanism for a cohort of neurodegenerative diseases. Neurobiol Aging 21:815–828.

Iida H, Shibata Y (1991) Functional Golgi units in microtubule-disrupted cultured atrial myocytes. J Histochem Cytochem 39:1349–1355.

Irizarry MC, Growdon W, Gomez-Isla T, Newell K, George JM, Clayton DF, Hyman BT (1998) Nigral and cortical Lewy bodies and dystrophic nigral neurites in Parkinson's disease and cortical Lewy body disease contain alpha-synuclein immunoreactivity. J Neuropathol Exp Neurol 57:334–337.

Iseki E, Marui W, Sawada H, Ueda K, Kosaka K (2000) Accumulation of human alpha-synuclein in different cytoskeletons in Lewy bodies in brains of dementia with Lewy bodies. Neurosci Lett 290:41–44.

Iwata-Ichikawa E, Kondo Y, Miyazaki I, Asanuma M, Ogawa N (1999) Glial cells protect neurons against oxidative stress via transcriptional up-regulation of the glutathione synthesis. J Neurochem 72:2334–2344.

Jellinger KA (2003) General aspects of neurodegeneration. J Neural Transm (Suppl) 65:101–144.

Johnston JA, Ward CL, Kopito RR (1998) Aggresomes: a cellular response to misfolded proteins. J Cell Biol 143:1883–1898.

Kawamura K, Izumi H, Ma Z, Ikeda R, Moriyama M, Tanaka T, Nojima T, Levin LS, Fujikawa-Yamamoto K, Suzuki K, Fukasawa K (2004) Induction of centrosome amplification and chromosome instability in human bladder cancer cells by p53 mutation and cyclin E overexpression. Cancer Res 64:4800–4809.

Kopito RR (2000) Aggresomes, inclusion bodies and protein aggregation. Trends Cell Biol 10:524–530.

Lacey KR, Jackson PK, Stearns T (1999) Cyclin-dependent kinase control of centrosome duplication. Proc Natl Acad Sci USA 96: 2817–2822.

Laser H, Mack TG, Wagner D, Coleman MP (2003) Proteasome inhibition arrests neurite outgrowth and causes "dying-back" degeneration in primary culture. J Neurosci Res 74:906–916.

Leask A, Obrietan K, Stearns T (1997) Synaptically coupled central nervous system neurons lack centrosomal gamma-tubulin. Neurosci Lett 229:17–20.

Lee HJ, Shin SY, Choi C, Lee YH, Lee SJ (2002) Formation and removal of alpha-synuclein aggregates in cells exposed to mitochondrial inhibitors. J Biol Chem 277:5411–5417.

Lee SS, Kim YM, Junn E, Lee G, Park KH, Tanaka M, Ronchetti RD, Quezado MM, Mouradian MM (2003) Cell cycle aberrations by alpha-synuclein over-expression and cyclin B immunoreactivity in Lewy bodies. Neurobiol Aging 24:687–696.

Letourneau PC, Wire JP (1995) Three-dimensional organization of stable microtubules and the Golgi apparatus in the somata of developing chick sensory neurons. J Neurocytol 24:207–223.

Lowenstein PR, Morrison EE, Bain D, Shering AF, Banting G, Douglas P, Castro MG (1994) Polarized distribution of the trans-Golgi network marker TGN38 during the in vitro development of neocortical neurons: effects of nocodazole and brefeldin A. Eur J Neurosci 6:1453–1465.

Marshall LE, Himes RH (1978) Rotenone inhibition of tubulin self-assembly. Biochim Biophys Acta 543:590–594.

Matsumoto K, Ohta T (1993) Mitosis of rotenone-induced endoreduplication in Chinese hamster cells. Jpn J Genet 68:185–194.

McNaught KS, Mytilineou C, Jnobaptiste R, Yabut J, Shashidharan P, Jennert P, Olanow CW (2002a) Impairment of the ubiquitin-proteasome system causes dopaminergic cell death and inclusion body formation in ventral mesencephalic cultures. J Neurochem 81:301–306.

McNaught KS, Shashidharan P, Perl DP, Jenner P, Olanow CW (2002b) Aggresome-related biogenesis of Lewy bodies. Eur J Neurosci 16:2136–2148.

Nagy Z, Esiri MM, Smith AD (1998) The cell division cycle and the pathophysiology of Alzheimer's disease. Neuroscience 87:731–739.

Nakao N, Nakai K, Itakura T (1997) Metabolic inhibition enhances selective toxicity of L-DOPA toward mesencephalic dopamine neurons in vitro. Brain Res 777:202–209.

Oakley CE, Oakley BR (1989) Identification of gamma-tubulin, a new member of the tubulin superfamily encoded by mipA gene of *Aspergillus nidulans*. Nature 338:662–664.

Olanow CW, Perl DP, DeMartino GN, McNaught KS (2004) Lewy-body formation is an aggresome-related process: a hypothesis. Lancet Neurol 3:496–503.

Olanow CW, Tatton WG (1999) Etiology and pathogenesis of Parkinson's disease. Annu Rev Neurosci 22:123–144.

Paglini G, Peris L, Diez-Guerra J, Quiroga S, Caceres A (2001) The Cdk5-p35 kinase associates with the Golgi apparatus and regulates membrane traffic. EMBO Rep 2:1139–1144.

Perier C, Bove J, Vila M, Przedborski S (2003) The rotenone model of Parkinson's disease. Trends Neurosci 26:345–346.

Pockwinse SM, Krockmalnic G, Doxsey SJ, Nickerson J, Lian JB, van Wijnen AJ, Stein JL, Stein GS, Penman S (1997) Cell cycle independent interaction of CDC2 with the centrosome, which is associated with the nuclear matrix-intermediate filament scaffold. Proc Natl Acad Sci USA 94:3022–3027.

Robinson MS (1990) Cloning and expression of gamma-adaptin, a component of clathrin-coated vesicles associated with the Golgi apparatus. J Cell Biol 111:2319–2326.

Rogalski AA, Singer SJ (1984) Associations of elements of the Golgi apparatus with microtubules. J Cell Biol 99:1092–1100.

Sakka N, Sawada H, Izumi Y, Kume T, Katsuki H, Kaneko S, Shimohama S, Akaike A (2003) Dopamine is involved in selectivity of dopaminergic neuronal death by rotenone. Neuroreport 14:2425–2428.

Sakurai A, Okamoto K, Fujita Y, Nakazato Y, Wakabayashi K, Takahashi H, Gonatas NK (2000) Fragmentation of the Golgi apparatus of the ballooned neurons in patients with corticobasal degeneration and Creutzfeldt-Jakob disease. Acta Neuropathol (Berl) 100: 270–274.

Sakurai A, Okamoto K, Yaguchi M, Fujita Y, Mizuno Y, Nakazato Y, Gonatas NK (2002) Pathology of the inferior olivary nucleus in patients with multiple system atrophy. Acta Neuropathol (Berl) 103:550–554.

Sathasivam K, Woodman B, Mahal A, Bertaux F, Wanker EE, Shima DT, Bates GP (2001) Centrosome disorganization in fibroblast cultures derived from R6/2 Huntington's disease (HD) transgenic mice and HD patients. Hum Mol Genet 10:2425–2435.

Sato N, Mizumoto K, Nakamura M, Ueno H, Minamishima YA, Farber JL, Tanaka M (2000) A possible role for centrosome overduplication in radiation-induced cell death. Oncogene 19:5281–5290.

Sawada H, Kohno R, Kihara T, Izumi Y, Sakka N, Ibi M, Nakanishi M, Nakamizo T, Yamakawa K, Shibasaki H, Yamamoto N, Akaike A, Inden M, Kitamura Y, Taniguchi T, Shimohama S (2004) Proteasome mediates dopaminergic neuronal degeneration, and its inhibition causes alpha-synuclein inclusions. J Biol Chem 279: 10710–10719.

Sherer TB, Betarbet R, Stout AK, Lund S, Baptista M, Panov AV, Cookson MR, Greenamyre JT (2002) An in vitro model of Parkinson's disease: linking mitochondrial impairment to altered alpha-synuclein metabolism and oxidative damage. J Neurosci 22: 7006–7015.

Sherer TB, Betarbet R, Kim JH, Greenamyre JT (2003a) Selective microglial activation in the rat rotenone model of Parkinson's disease. Neurosci Lett 341:87–90.

Sherer TB, Kim JH, Betarbet R, Greenamyre JT (2003b) Subcutaneous rotenone exposure causes highly selective dopaminergic degeneration and alpha-synuclein aggregation. Exp Neurol 179: 9–16.

Smith PD, Crocker SJ, Jackson-Lewis V, Jordan-Sciutto KL, Hayley S, Mount MP, O'Hare MJ, Callaghan S, Slack RS, Przedborski S, Anisman H, Park DS (2003) Cyclin-dependent kinase 5 is a mediator of dopaminergic neuron loss in a mouse model of Parkinson's disease. Proc Natl Acad Sci USA 100:13650–13655.

Spillantini MG, Schmidt ML, Lee VM, Trojanowski JQ, Jakes R, Goedert M (1997) Alpha-synuclein in Lewy bodies. Nature 388: 839–840.

Stearns T, Evans L, Kirschner M (1991) Gamma-tubulin is a highly conserved component of the centrosome. Cell 65:825–836.

Stieber A, Mourelatos Z, Gonatas NK (1996) In Alzheimer's disease the Golgi apparatus of a population of neurons without neurofibrillary tangles is fragmented and atrophic. Am J Pathol 148:415–426.

Sulimenko V, Sulimenko T, Poznanovic S, Nechiporuk-Zloy V, Bohm KJ, Macurek L, Unger E, Draber P (2002) Association of brain gamma-tubulins with alpha beta-tubulin dimers. Biochem J 365: 889–895.

Sunkel CE, Gomes R, Sampaio P, Perdigao J, Gonzalez C (1995) Gamma-tubulin is required for the structure and function of the microtubule organizing centre in *Drosophila* neuroblasts. EMBO J 14:28–36.

Tanaka M, Kim YM, Lee G, Junn E, Iwatsubo T, Mouradian MM (2004) Aggresomes formed by alpha-synuclein and synphilin-1 are cytoprotective. J Biol Chem 279:4625–4631.

Trojanowski JQ, Goedert M, Iwatsubo T, Lee VM (1998) Fatal attractions: abnormal protein aggregation and neuron death in Parkinson's disease and Lewy body dementia. Cell Death Differ 5:832–837.

Trushina E, Heldebrant MP, Perez-Terzic CM, Bortolon R, Kovtun IV, Badger JD 2nd, Terzic A, Estevez A, Windebank AJ, Dyer RB, Yao J, McMurray CT (2003) Microtubule destabilization and nuclear entry are sequential steps leading to toxicity in Huntington's disease. Proc Natl Acad Sci USA 100:12171–12176.

Waelter S, Boeddrich A, Lurz R, Scherzinger E, Lueder G, Lehrach H, Wanker EE (2001) Accumulation of mutant huntingtin fragments in aggresome-like inclusion bodies as a result of insufficient protein degradation. Mol Biol Cell 12:1393–1407.

Wagner M, Rajasekaran AK, Hanzel DK, Mayor S, Rodriguez-Boulan E (1994) Brefeldin A causes structural and functional alterations of the trans-Golgi network of MDCK cells. J Cell Sci 107:933–943.

Wakabayashi K, Hayashi S, Yoshimoto M, Kudo H, Takahashi H (2000) NACP/alpha-synuclein-positive filamentous inclusions in astrocytes and oligodendrocytes of Parkinson's disease brains. Acta Neuropathol (Berl) 99:14–20.

Wigley WC, Fabunmi RP, Lee MG, Marino CR, Muallem S, DeMartino GN, Thomas PJ (1999) Dynamic association of proteasomal machinery with the centrosome. J Cell Biol 145:481–490.

Yamada T, Akiyama H, McGeer PL (1991) Two types of spheroid bodies in the nigral neurons in Parkinson's disease. Can J Neurol Sci 18:287–294.

Yang Y, Geldmacher DS, Herrup K (2001) DNA replication precedes neuronal cell death in Alzheimer's disease. J Neurosci 21:2661–2668.

Yu W, Centonze VE, Ahmad FJ, Baas PW (1993) Microtubule nucleation and release from the neuronal centrosome. J Cell Biol 122:349–359.

Zheng Y, Jung MK, Oakley BR (1991) Gamma-tubulin is present in *Drosophila melanogaster* and *Homo sapiens* and is associated with the centrosome. Cell 65:817–823.

Zmuda JF, Rivas RJ (1998) The Golgi apparatus and the centrosome are localized to the sites of newly emerging axons in cerebellar granule neurons in vitro. Cell Motil Cytoskeleton 41:18–38.

(Accepted 26 January 2005)
(Available online 24 March 2005)

The FASEB Journal express article 10.1096/fj.05-4996fje. Published online January 10, 2006.

Methamphetamine-induced dopaminergic neurotoxicity is regulated by quinone formation-related molecules

Ikuko Miyazaki,* Masato Asanuma,* Francisco J. Diaz-Corrales,* Masaya Fukuda,† Kiyoyuki Kitaichi,† Ko Miyoshi,* and Norio Ogawa*

*Department of Brain Science, Okayama University Graduate School of Medicine, Dentistry and Pharmaceutical Sciences, Okayama, Japan; and †Department of Medical Technology, Nagoya University Graduate School of Medicine, Nagoya, Japan

Corresponding author: Masato Asanuma, Department of Brain Science, Okayama University Graduate School of Medicine, Dentistry and Pharmaceutical Sciences, Okayama, Japan. E-mail: asachan@cc.okayama-u.ac.jp

ABSTRACT

Recently, the neurotoxicity of dopamine (DA) quinone formation by auto-oxidation of DA has focused on dopaminergic neuron-specific oxidative stress. In the present study, we examined DA quinone formation in methamphetamine (METH)-induced dopaminergic neuronal cell death using METH-treated dopaminergic cultured CATH.a cells and METH-injected mouse brain. In CATH.a cells, METH treatment dose-dependently increased the levels of quinoprotein (protein-bound quinone) and the expression of quinone reductase in parallel with neurotoxicity. A similar increase in quinoprotein levels was seen in the striatum of METH (4 mg/kg X4, i.p., 2 h interval)-injected BALB/c mice, coinciding with reduction of DA transporters. Furthermore, pretreatment of CATH.a cells with quinone reductase inducer, butylated hydroxyanisole, significantly and dose-dependently blocked METH-induced elevation of quinoprotein, and ameliorated METH-induced cell death. We also showed the protective effect of tyrosinase, which rapidly oxidizes DA and DA quinone to form stable melanin, against METH-induced dopaminergic neurotoxicity in vitro and in vivo using tyrosinase null mice. Our results indicate that DA quinone formation plays an important role, as a dopaminergic neuron-specific neurotoxic factor, in METH-induced neurotoxicity, which is regulated by quinone formation-related molecules.

Key words: dopamine quinone • quinone reductase • tyrosinase

Methamphetamine (METH) is a drug of abuse that causes damage to striatal dopaminergic and serotonergic nerve terminals (1–3). Various hypotheses regarding the mechanism responsible for METH-induced neurotoxicity has been proposed (4–14); however, the exact mechanism responsible for METH-induced striatal dopaminergic neurotoxicity remains unclear. Several studies have demonstrated that endogenous dopamine (DA) plays an important role in mediating METH-induced neuronal damage (6, 9, 12, 13). DA release and redistribution from synaptic vesicles to cytoplasmic compartments and consequent

elevation of cytosolic oxidizable DA concentrations are thought to be related to DA terminal injury induced by METH exposure (6). Reactive oxygen species (ROS) such as superoxide and hydroxyl radicals, generated by auto-oxidation of cytosolic-free DA, appear to be involved in METH-induced dopaminergic neuronal damage (5). Using vesicular monoamine transporter (VMAT)-2 knockout mice, Fumagalli et al. (7) showed that disruption of VMAT potentiates METH-induced neurotoxicity in vivo and point to a greater contribution of intraneuronal DA redistribution rather than extraneuronal overflow on mediating this effect. Furthermore, LaVoie and Hastings (8) demonstrated that increased intracellular DA oxidation is associated with METH neurotoxicity by measuring 5-cysteinyl-DA, a product of DA quinone bound to cysteinyl residue on protein, but not extracellular DA. In contrast, another hypothesis suggests that METH-induced DA release, consequently elevating extracellular DA concentrations, is responsible for METH-induced neurotoxicity (4, 10, 11). In addition, Yuan et al. (14) questioned the view that endogenous DA plays an essential role in METH-induced DA neurotoxicity. Although there is a controversy regarding the mechanism through which METH produces its neurotoxic effects, there is general agreement that DA plays a role in METH neurotoxicity.

DA is stable in the synaptic vesicle under normal physiological conditions. However, excessive levels of cytosolic DA outside the vesicles in damaged DA neurons is thought to induce neurotoxicity through the generation of ROS and reactive DA quinones (15, 16). The generated DA quinones covalently conjugate with the sulfhydryl group of cysteine on functional proteins (17, 18), resulting predominantly in the formation of 5-cysteinyl-DA (15, 19). The formed 5-cysteinyl-DA irreversibly alters protein function and consequently causes DA neuron-specific cytotoxicity (8, 20). DA-induced formation of DA quinones and the consequent dopaminergic cell damage in vitro and in vivo were successfully prevented by treatment with superoxide dismutase, glutathione, and some thiol reagents through their quinone-quenching activities (8, 17, 21–24). Recently, the neurotoxicity of DA quinone formation by auto-oxidation of DA has turned the focus on dopaminergic neuron-specific oxidative stress (25, 26).

A multifunctional enzyme, tyrosinase (EC 1.14.18.1; monophenol monooxygenase), catalyzes both the hydroxylation of tyrosine to L-DOPA and the consequent oxidation of L-DOPA to form melanin in the melanin biosynthesis pathway (27). Furthermore, tyrosinase oxidizes not only L-DOPA but also DA to form melanin via the DA quinone (28). Some studies have revealed that tyrosinase, tyrosinase promoter activity, and tyrosinase-like activity are also expressed in the central nervous system (29–34). Tyrosinase in the brain may enzymatically and rapidly oxidize excess amounts of cytosolic DA to form stable melanin, which may consequently prevent the slow progression of cell damage induced by DA auto-oxidation and long-term exposure to DA quinone.

The present study was designed to further examine the mechanism of METH-induced dopaminergic neurotoxicity using METH-treated dopaminergic cells and METH-injected mouse brain. The results confirmed the involvement of quinoprotein formation, which represents generation of DA quinones, in METH-induced dopaminergic neurotoxicity. The results also demonstrated the protective effect of tyrosinase, which rapidly oxidizes DA and DA quinone to form stable melanin, against METH-induced dopaminergic neurotoxicity.

MATERIALS AND METHODS

Cell culture

Dopaminergic CATH.a cells (ATCC; #CRL-11179), derived from mouse DA-containing neurons, were cultured at 37°C in 5% CO_2 in RPMI 1640 culture medium (Invitrogen, San Diego, CA) supplemented with 4% fetal bovine serum, 8% horse serum, 100 U/ml penicillin and 100 μg/ml streptomycin. Cells were seeded in 96-well culture plates (Becton Dickinson Labware, Franklin Lakes, NJ) for the measurement of cell toxicity, in 6-well plates for the extraction of total cell lysates used for the measurement of protein-bound quinone and Western blot analysis at a density of 1.0×10^5 cells/cm^2. After 24 h, cells were treated with METH and/or other drugs.

Animal experiments

Male BALB/c mice (9 weeks old; Charles River Japan Inc., Yokohama, Japan), albino tyrosinase null C57BL/6J-Tyr$^{c\text{-}2J}$/Tyr$^{c\text{-}2J}$ mice, which have spontaneous mutation in tyrosinase gene (9 wk old; Jackson Laboratories, Bar Harbor, ME), and their wild-type C57BL/6J mice were used in the present study. All animal procedures were conducted in strict accordance with "The Guidelines for Animal Experiments" at Okayama University Medical School. Mice were repeatedly injected with METH (4 mg/kg×4, i.p. with 2-h intervals) or saline, and used for assay of protein-bound quinone formation or immunohistochemistry.

LDH assay for measurement of cell toxicity

CATH.a cells were exposed to 1–4 mM METH diluted in H_2O for 24 h with/without pretreatment with 25–100 μM butylated hydroxyanisol (BHA) for 6 h or simultaneous treatment with 50–250 μM phenylthiourea (PTU), a tyrosinase inhibitor. Cell toxicity was determined by measuring lactate dehydrogenase (LDH) release (whole isozyme) from treated cells. LDH assays (Wako Pure Chemical Industries, Osaka, Japan) were performed as reported previously (35) and in accordance with the instructions supplied by the manufacturer. In brief, the culture medium from cells treated with drugs was added to the enzymatic reaction buffer containing lithium lactate, NAD, diaphorase, and nitro blue tetrazolium dye and incubated for 20 min at room temperature. Absorption values at 560 nm were measured to determine levels of released LDH. The culture medium from cells treated with Tween-20 for 30 min was used as a positive control.

Measurement of protein-bound quinone (quinoprotein)

CATH.a cells were exposed to 1–4 mM METH diluted in H_2O for 24 h with/without pretreatment with 25–100 μM BHA for 6 h, 1 μM reserpine or 100 μM α-methyl-*p*-tyrosine (α-MT) for 24 h before extraction of total cell lysates. For BALB/c mice injected with METH, total cell lysates were extracted from the striatum of mice 1, 3, and 14 days after the last METH injection. Total cell lysates were prepared with 10 μg/ml phenylmethylsulfonyl fluoride (Sigma Chemical Co., St. Louis, MO) in ice-cold-RIPA buffer [phosphate buffer saline; PBS (pH 7.4), 1% NP-40, 0.5% sodium deoxycholate and 0.1% sodium dodecyl sulfate]. For detection of protein-bound quinones (quinoprotein), the NBT/glycinate assay was performed as described previously (36). The lysates were used for the NBT/glycinate colorimetric assay. The protein sample was added to 500 ml of NBT reagent (0.24 mM NBT in 2 M potassium glycinate, pH

10.0) followed by incubation in the dark for 2 h on a shaker. The absorbance of blue-purple color developed in the reaction mixture was measured at 530 nm.

Western blot analysis

CATH.a cells were pretreated with 50 μM BHA for 6 h and subsequently cotreated with 2 mM METH for 24 h. Total cell lysate was extracted from treated cells with RIPA buffer containing 10 μg/ml phenylmethylsulfonyl fluoride. Western blot analysis was performed as described previously (37). In brief, protein samples (10 μg) were loaded on 12.5% sodium dodecyl sulfate (SDS) polyacrylamide gels and blotted onto nitrocellulose membranes (Hybond ECL, Amersham, Buckinghamshire, UK). Blots were incubated with goat anti-NQO-1 (1: 200 dilution, Santa Cruz Biotechnology, Santa Cruz, CA), and then reacted with donkey anti-goat (1:5000 dilution, Chemicon, Temecula, CA) secondary antibody conjugated to horseradish peroxidase. After washing with 20 mM Tris-buffered saline containing 0.1% Tween-20, blots were developed using the ECL Western blotting detection system (Amersham). For quantitative analysis, the ratio for NQO-1 protein (relative density of the signal) and the constitutively expressed β-actin protein were calculated to normalize for loading and transfer artifacts introduced in Western blotting.

Tissue preparation for immunohistochemistry

Mice were transcardially perfused with saline followed by a fixative containing 4% paraformaldehyde, 0.35% glutaraldehyde in 0.1 M phosphate buffer (PB, pH 7.4) under pentobarbital sodium anesthesia (70 mg/kg, i.p.) 1, 3, and 14 days after treatment of BALB/c, $Tyr^{c\text{-}2J}/Tyr^{c\text{-}2J}$ or C57BL/6J mice with METH or saline. After the perfusion, the brains were rapidly removed en bloc from the skull, postfixed for 24 h in a fixative containing 4% paraformaldehyde in 0.1M PB (pH 7.4) and then cryoprotected in 15% sucrose in PB for ~48 h. Brain snap-frozen with powdered dry ice was cut coronally on a cryostat at levels containing the striatum at 20-μm thickness. Sections were collected in 10 mM PBS with 0.1% sodium azide until staining. All the above procedures were carried out at 4°C.

Immunohistochemistry

DA transporter (DAT)-immunopositive cells in the striatum were stained by standard immunohistochemistry. The sections were soaked overnight in 10 mM PBS containing 0.2% Triton X-100 (PBST) before incubation in 0.5% H_2O_2 in PBST for 30 min at room temperature. After washing with PBST (5×5 min), the sections were incubated in 1% normal rabbit serum in PBST for 30 min, and exposed to anti-DAT goat polyclonal antibody (diluted 1:200 in PBST; Santa Cruz Biotechnology) for 18 h at 4°C. After incubation with the primary antibody, sections were washed for 5 × 5 min in PBST before incubation with biotinylated rabbit anti-goat IgG secondary antibody (diluted 1:1,000 in PBST: Vector Laboratories, Burlingame, CA) for 2 h at room temperature. After washes in PBST (3×10 min), the sections were incubated with the avidin-biotin peroxidase complex (diluted 1:2,000, Vector Laboratories) for 1 h at room temperature. DAT-immunopositive cells were visualized by 3,3′-diaminobenzidine (DAB), nickel, and H_2O_2.